AADE-14-FTCE-45

Transport of Soluble Drilled Cuttings

Fabio Silva, Federal U of Rio de Janeiro; Luiz Calçada, Federal Rural U of Rio de janeiro, André Martins,Petrobras

Abstract

Drilling massive salt zones became a routine in the development of the sub-salt reservoirs offshore Brazil. In this scenario, typical wells frequently include drilling of 2000m of salt zones with non-aqueous fluids. Due to cuttings discharge regulations, cutting drying processes must be used, which limit drilling performance. One alternative to enhance the process efficiency is to use saturated water based fluids which would not require cuttings drying operations. The adoption of this technique requires special care with wellbore leaching and stability issues, but seems very attractive. This article deals with the design of hydraulic parameters to guarantee proper salt cuttings transport. Since the cuttings are soluble in the drilling fluid (which is subsaturated in downhole conditions) its diameter decrease with the flow, increasing the tolerance to cuttings concentration for a constant downhole pressure. As a consequence, ROP limits are loosened and safe hole cleaning can be achieved even at high ROPs. The design process is based at a coupled mass/ momentum transfer model to account for the physics involved.

Introduction

Offshore drilling is associated with extremely high costs and any effort on design and well construction optimization is welcome to reduce drilling time. Massive salt drilling is a major concern in several offshore operations in the Brazilian coast: the development of pre-salt fields frequently require wells crossing salt zones as long as 2000m.

A few hundred wells have already been drilled in the zone and the learning curve was fast enough to accomplish high ROPs in the salt. The phase is normally drilled with 17 ½ in bits and NAF systems. The choice for the organic phase fluid is convenient in several aspects, including salt leaching prevention, lubricity and stuck pipe remediation strategies. On the other hand, cost, logistic issues and cuttings treatment requirements impose several constraints. Today, the main restriction for ROP enhancement in the 17 ½ in phase is associated with poor behavior of the cuttings separation/drying system. Obviously, upgrading the systems in offshore vessels is a requirement but downtimes associated with equipment substitution always postpone the task.

Drilling salt zones with nearly saturated water based fluid appear as an interesting option in several cases (Lomba[10], R. F. et al., 2013). In other scenarios, drilling with sea water may be a feasible and low cost option (Wilson[18], S. M. et al., 2004). In this scenario, understanding salt leaching is a requirement and some modeling effort have been spent and an adequate design software provided (Folsta[7], M. G. et al., 2013).

Drilling formations which solubilize in the drilling fluid may be convenient for hole cleaning and hydraulic design since cuttings tend to disappear while being transported from the bottomhole to surface. This fact motivates the proper understanding of the physics involved in order to produce less conservative well designs (pushing ROP limits at lower flow rates).

Objectives

The main goal of this study is to provide a mathematical formula to characterize the transportation of soluble drilled cuttings. This formulation should take into account relevant design parameters, such as ROP, salt concentration in the drilling fluid and fluid viscosity.

Formulation

Figure 1 illustrates the force balance acting on a particle falling on a stationary fluid, including weight (W), buoyancy (B) and drag (D). Traditional Stokes approach solves the force balance for the equilibrium condition, where a terminal velocity is reached.

In the proposed problem, however, the particle is soluble in the fluid. Consequently its diameter will be continuously reduced resulting that the particle velocity will not be reached (unless the particle is totally dissolved). Since the force balance will not reach the equilibrium, Eq. (1), known as Newton second law, will be adopted to represent the phenomena.

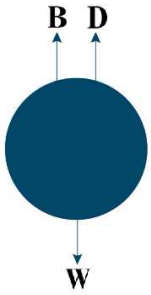

Figure 1 – Free-body diagram.

$$W - D - B = m_p \frac{dv}{dt} \quad (1)$$

Where m_p is the particle mass and dv/dt is its acceleration.

At a first moment, the settling velocity behavior without the influence of inertia term, in other words, considering that the particle acceleration can be neglected. Due to this, the equation to the sphere particle is thus defined:

$$W - D - B = 0 \quad (2)$$

The sphere weight (W) is defined as:

$$W = m_p g \quad (3)$$

Where g is the gravity acceleration.

The buoyancy (B) force exerted by the fluid on the particle, considering that the particle volume is equal to the displaced fluid volume, is:

$$B = \rho_f g V_p \quad (4)$$

Where ρ_f is the fluid specific mass and V_p is the sphere volume, that is defined as:

$$V_p = \frac{\pi d_p^3}{6} \quad (5)$$

Where d_p is the particle diameter.

And, finally, the following equation is used for the drag force by definition:

$$D = \frac{\rho_f v_\infty^2 A C_D}{2} \quad (6)$$

Where v_∞ is the isolated particle settling velocity, C_D is the drag coefficient and A is a characteristic area, which is the cross-sectional area of the sphere given by:

$$A = \frac{\pi d_p^2}{4} \quad (7)$$

Substituting Eq. (7) into Eq. (6):

$$D = \frac{\rho_f v_\infty^2 \pi d_p^2 C_D}{8} \quad (8)$$

Substituting Eqs. (3), (4) and (8) into Eq. (2), we obtain:

$$m_p g - \frac{\rho_f v_\infty^2 \pi d_p^2 C_D}{8} - \rho_f g V_p = 0 \quad (9)$$

But,

$$m_p = \rho_p V_p \quad (10)$$

Where ρ_p is the particle specific gravity:

Substituting Eq. (10) into Eq. (9):

$$\rho_p V_p g - \frac{\rho_f v_\infty^2 \pi d_p^2 C_D}{8} - \rho_f g V_p = 0 \quad (11)$$

Substituting Eq. (5) into Eq. (11), we have:

$$\frac{g \pi d_p^3}{6}\left(\rho_p - \rho_f\right) - \frac{\rho_f v_\infty^2 \pi d_p^2 C_D}{8} = 0 \quad (12)$$

Solving for the settling velocity:

$$v_\infty = \sqrt{\frac{4g(\rho_p - \rho_f)d_p}{3\rho_f C_D}} \quad (13)$$

If the inertia term is considered, similar development will lead to the following equation:

$$\frac{d(v_\infty)}{dt} = \frac{g\left(\rho_p - \rho_f\right)}{\rho_p} - \frac{3\rho_f v_\infty^2 C_D}{4\rho_p d_p} \quad (14)$$

Additional information is required to solve either Eq. (13) or Eq. (14): the proper characterization of drag phenomena and of the dissolution rates of the cutting in the fluid. These topics are addressed in the following items.

Drag Coefficient Calculation

The model proposed for drag coefficients adopted in this work was the one proposed by Coelho and Massarani[5] (1996) correlation based on data of Lapple and Shepherd[8] (1940) and Pettjohn and Christiansen[14] (1948), as follows:

$$C_D = \left[\left(\frac{24}{\mathrm{Re}}\right)^{0,63} + 0.43^{0,63}\right]^{\frac{1}{0,63}} \quad (15)$$

This correlation is valid for Reynolds number lower than fifty thousand. The Reynolds number is defined as follows:

$$\mathrm{Re} = \frac{\rho_f V_t d_P}{\eta_a} \quad (16)$$

Where Re is the Reynolds number, v_t is the transport velocity and η_a is the apparent viscosity.

The apparent viscosity will be evaluated by the power law model, as follows:

$$\eta_a = K \dot{\gamma}^{n-1} \quad (17)$$

Where K is the fluid consistent index, n is the flow behavior index and γ is the shear rate. The shear rate should be evaluated at the particle transport velocity, in order to account for shear thinning behavior due to fluid pumping. The transport velocity of the cuttings toward the surface is defined by:

$$v_t = v_f - v_p \quad (18)$$

Where v_f is the fluid velocity and v_p is the particle velocity.

Particle diameter decay calculation

The next step would be to characterize the decrease in particle diameter due to its dissolution in the fluid.

According to Aksel'rud[1] et al. (1992), it is performed the following mass balance in an isolated soluble particle immersed into a fluid.

$$\frac{d(m_p)}{dt} = -ka(C^* - C) \quad (19)$$

Where t is the time, k is the mass transfer coefficient, C^* is the saturation concentration of NaCl in water, C is the instantaneous concentration of the solution and a is the surface area of the spherical particle that is defined as follows:

$$a = \pi d_p^2 \quad (20)$$

Substituting Eqs. (10) and (20) into Eq. (19):

$$\rho_p \frac{d(V_P^3)}{dt} = -k\pi d_p^2 (C^* - C) \quad (21)$$

Now, substituting Eq. (5) into Eq. (21):

$$\rho_P \frac{\pi}{6} \frac{d(d_p^3)}{dt} = -k\pi d_p^2 (C^* - C) \quad (22)$$

Joining the constant value parameters to simplify last equation:

$$\frac{d(d_p^3)}{dt} = -bd_p^2 \quad (23)$$

Where b is a constant parameter defined as follows:

$$b = k\frac{6}{\rho_p}(C^* - C) \quad (24)$$

To facilitate integration, the follow substitution is performed:

$$y = d_p^3 \quad (25)$$

Eq. (23) turns into:

$$\frac{dy}{dt} = -by^{\frac{2}{3}} \quad (26)$$

Integrating:

$$3y^{\frac{1}{3}} = -bt + C1 \quad (27)$$

Where C1 is the integration constant.

Returning to the substitution shown in Eq. (25):

$$3d_P = -bt + C1 \quad (28)$$

Initial condition: $d_p = d_{p_0}$ in t = 0.

Where d_{p0} is the initial diameter.

Thus, the constant integration value is known:

$$C1 = 3d_{p_o} \quad (29)$$

Eq. (28) turns into:

$$d_p = -\frac{bt}{3} + d_{p_0} \quad (30)$$

Returning to the substitution shown in Eq. (25):

$$d_p = d_{p_0} - 2\frac{k}{\rho_p}(C^* - C)t \quad (31)$$

Population/ wall Effects on Particle Sedimentation

Both the presence of additional particles and walls confining the flow impose additional barriers to particle sedimentation.

In this study, the correlation of Richardson and Zaki[17] (1954) for the settling velocity correction of rounded particles will be used to account for particle concentration (population effect). U is the corrected velocity.

$$\frac{U}{v_\infty} = f(\mathrm{Re}, \varepsilon) \tag{32}$$

Where ε is the fluid volumetric fraction in suspension, which is defined as follows:

$$\varepsilon = 1 - cv \tag{33}$$

Where cv is the solids volumetric fraction in suspension just above the bit.

The correlation is presented as follows:

$$\frac{U}{v_\infty} = \varepsilon^m \tag{34}$$

m is a function of Reynolds number, as shown in Table 1:

Table 1 – m values according to Reynolds number.

Re	m
<0.2	3.65
0.2-1	$4.35\,\mathrm{Re}_\infty^{-0.03} - 1$
1-500	$4.45\,\mathrm{Re}_\infty^{-0.1} - 1$
>500	1.39

The fluid dynamics of the particle is influenced by the presence of rigid boundaries. Their effect results in a reduction in the isolated particle terminal velocity.

The correlation proposed by Almeida[2] (1995) was used for calculating the wall effect on the fluid dynamics of isometric particles. This model is limited to particles is in a range of sphericity, Φ, between 0.65 and 1 and the ratio between the particle diameter and the pipe diameter, d_p/d_t between zero and 0.5.

The corrected velocity for the wall effect, v_w, relates to the isolated particle terminal velocity as follows:

$$\frac{v_w}{v_\infty} = k_p \tag{35}$$

Where k_p is the correlation factor that corrects the settling velocity for that effect.

For Reynolds numbers smaller than 0.1, Francis[6] (1933) proposes the following correlation:

$$k_p = \left(\frac{1-\beta}{1-0.475\beta}\right)^4 \tag{36}$$

For Reynolds number larger than 1000, Munroe[13] (1888) proposes:

$$k_p = 1 - \beta^{1.5} \tag{37}$$

For an intermediate range of Reynolds number between 0.1 and 1000, Almeida[2] (1995) proposes:

$$k_p = \frac{10}{1 + A\,\mathrm{Re}_\infty^B} \tag{38}$$

Where:

$$A = 8.91e^{2.79\beta} \tag{39}$$

$$B = 1.17 * 10^{-3} - 0.281\beta \tag{40}$$

$$\beta = \frac{d_p}{d_h} \tag{41}$$

Where d_h is the hydraulic diameter, defined as follows:

$$d_h = 0.816(d_e - d_i) \tag{42}$$

Where d_e is the well diameter and d_i is the pipe external diameter.

Results

The software Mathematica 9 was used to perform simulations aiming the representation of the particle diameter decay of a soluble particle being transported in the wellbore annulus. This phenomenon interferes in its settling velocity and thus in its transport velocity. The influences of particles concentration in the fluid and the wall effects were also analyzed.

The simulations were carried out considering an incompressible shear thinning fluid, at a temperature of 30°C, Halite (NaCl) as the salt rock formation. This model was solved considering spherical particles moving at Reynolds numbers smaller than thirty.

Variable Diameter Behavior

Table 2 shows relevant parameter values considered in the simulations:

Table 2 – Data for the calculation of the variable particle diameter.

Parameters	Values
k (m/s)	10^{-4}
d_{p0} (in)	0.15
C^* (kg/m³)	315.15
C (kg/m³)	90
ρ_p (kg/m³)	2200

Figure 2 illustrates the decay of particle diameter with time

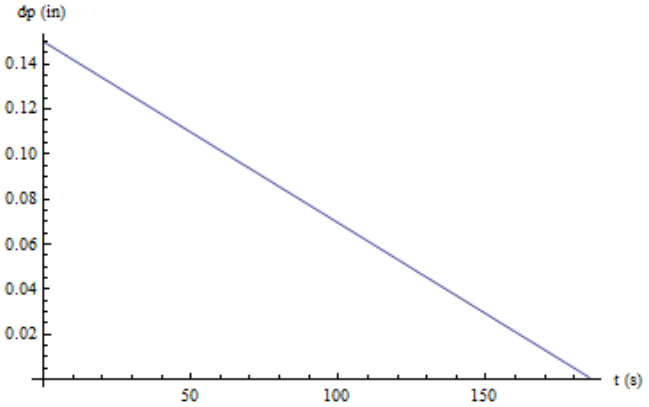

Figure 2 – Particle diameter (in) versus Time (s).

In this case, the particle generated by the bit with 0.15 in diameter dissolves completely in approximately 185 seconds.

Eq. (31) presents an analytical solution. The Mathematica program solved it directly, by entering the parameters values related to the particle, such as its initial diameter, its specific gravity and its mass transfer coefficient.

Some important observations were concluded from this result:

- The higher the initial salt particle diameter the longer will be its dissolution time;
- The higher the instantaneous concentration of salt in solution the larger will be the particle dissolution time;
- A higher mass transfer coefficient results in a shorter dissolution time;
- A higher particle specific gravity delays particle dissolution.

Comparison of Solutions with and without the Inertia Term

As explained previously, the particle terminal velocity is not reached because it is soluble in the drilling fluid, which will be shown in this section.

In this section, the solutions of the particle settling velocity equations without considering the inertia term, Eq. (13), and considering the inertia term, Eq. (14) will be compared. The data shown in Table 3 were used in the simulations.

Table 3 – Data for the calculation of the particle settling velocity.

Parameters	Values
g (m/s²)	9.81
ρ_p (kg/m³)	2200
ρ_f (kg/m³)	1199
K (Pa.s^n)	2.63
n	0.6
d_e (in)	17.5
d_i (in)	5
Q_f (gpm)	900

With the data from Table 3 and Eq. (29) solved, it is also necessary to incorporate the Eq. (18) for the solution of the particle settling velocity.

Eq. (18) is dependent on the Eq. (15), which is dependent on the Eqs. (16) and (17). Therefore, Eq. (15) turns into:

$$\mathrm{Re} = \frac{\rho_f (v_f - v_p) d_p}{K \dot{\gamma}^{n-1}} \tag{43}$$

The shear rate in relation to the particle is defined as follows:

$$\dot{\gamma} = \frac{(v_f - v_p)}{d_p} \tag{44}$$

The fluid velocity is given by:

$$v_f = \frac{4Q_f}{\pi(d_e^2 - d_i^2)} \tag{45}$$

Where Q_f is the injected fluid flow rate.

Substituting Eqs. (44) and (45) into Eq. (43):

$$\mathrm{Re} = \frac{\rho_f \left(\frac{4Q_f}{\pi(d_e^2 - d_i^2)} - v_p \right)^{2-n} d_p^n}{K} \tag{46}$$

Finally, we note that when substituting Eq. (18), which is solely dependent on the Eq. (46), into Eqs. (13) and (14), iterative solution will be required. Eq. (13), analytical was solved by a trial and error approach while Eq. (14) required numerical solution aided by NSOLVE functions.

Figure 3 show similar results for both solutions, indicating that the inertia term is negligible in the range of the interest of the present application.

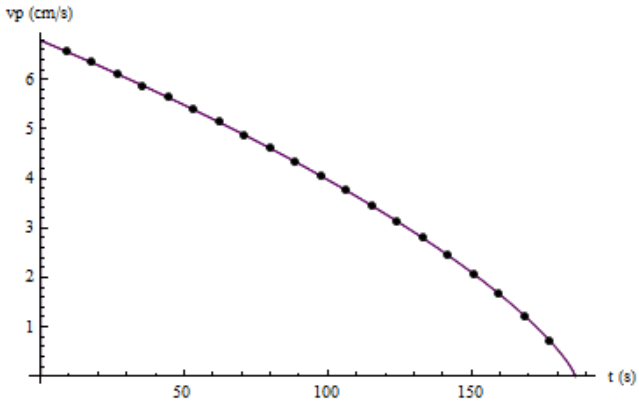

Figure 3 – Settling velocity (cm/s) versus Time (s). The purple curve drawn is from Equation (15). While the dotted curve corresponds to Equation (14).

An important observation to state from the results is that the difference between the specific gravities is the driving force for particle sedimentation and transport.

Relevant design parameter influence on cuttings transport will be presented in the next items.

Influence of Fluid Flow Rate

Two different wellbore diameters were considered (12 ¼ and 17 ½ in) and its typical flow rates. The following results (Figures 4 and 5) consider the sedimentation of an isolated particle.

- Phase $12^{1/4}$" x 5"

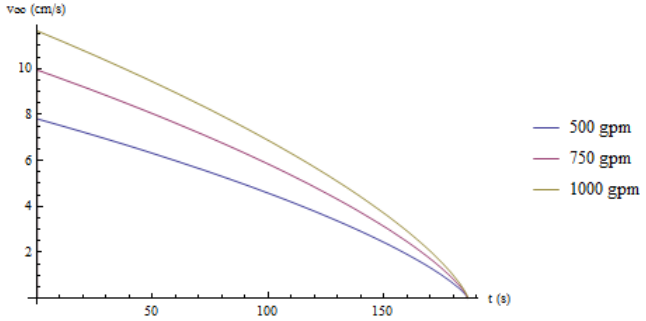

Figure 4 – Settling velocity (cm/s) versus Time (s), for phase $12^{1/4}$" x 5".

- Phase $17^{1/2}$" x 5"

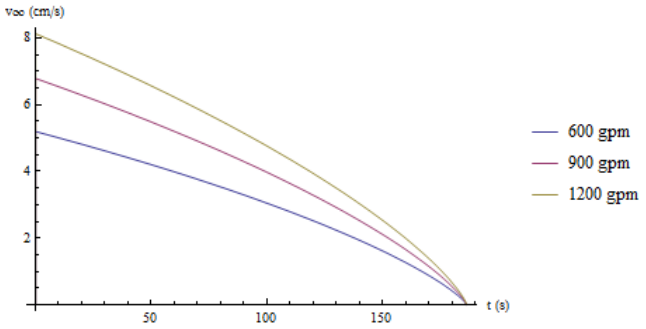

Figure 5 – Settling velocity (cm/s) versus Time (s), for phase $17^{1/2}$" x 5".

From these results it can be seen that the particle settling velocity increases as the annular space narrows possibly due to viscosity decrease in shear thinning fluids.

For a given well phase, when an increase in the injected fluid flow rate occurs, the fluid velocity increases, according to the continuity equation. Thus, the Reynolds number also increases, which causes a decrease in the drag coefficient of the particle, generating a higher settling velocity on it. Again shear thinning effects also rule results.

The following figures 6 and 7 reflect results for a given phase and flow rate of different sedimentation velocity approaches (single particle, population and wall effects). In all cases a minor effect in dissolution times was observed.

- Phase $12^{1/4}$" x 5", 750 GPM

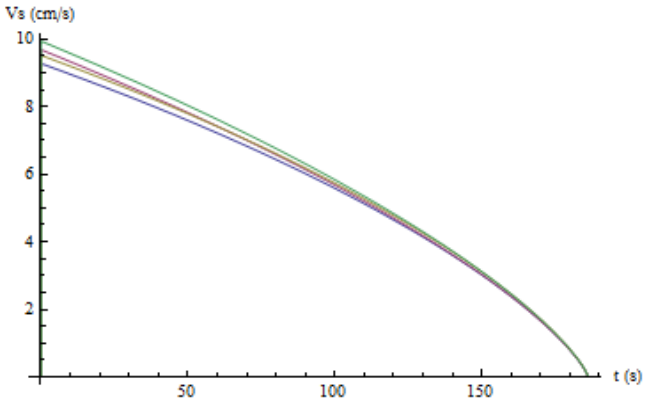

Figure 6 – Corrected settling velocity (cm/s) versus Time (s), for phase $12^{1/4}$" x 5". The green curve drawn is the uncorrected velocity. The pink curve is the corrected velocity by particles concentration effect. The yellow curve is the corrected velocity by wall effect. While the blue curve corresponds to the corrected velocity by both effects.

- Phase $17^{1/2}$" x 5" – 900 GPM

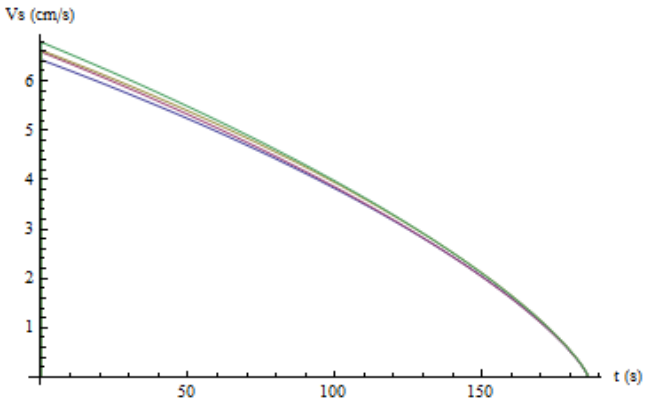

Figure 7 – Corrected settling velocity (cm/s) versus Time (s), for phase $17^{1/2}$" x 5". The green curve drawn is the uncorrected velocity. The pink curve is the corrected velocity by particles concentration effect. The yellow curve is the corrected velocity by wall effect. While the blue curve corresponds to the corrected velocity by both effects.

Besides a transport velocity (Eq. 18), a transport ratio can be defined by:

$$R_t = \frac{v_t}{v_f} = 1 - \frac{v_p}{v_f} \qquad (47)$$

The following figures 8 to 11 show the effect of particle dissolution on velocity transport and transport ratios for the two wellbore diameters under study

- Phase $12^{1/4}$" x 5" – 750 GPM

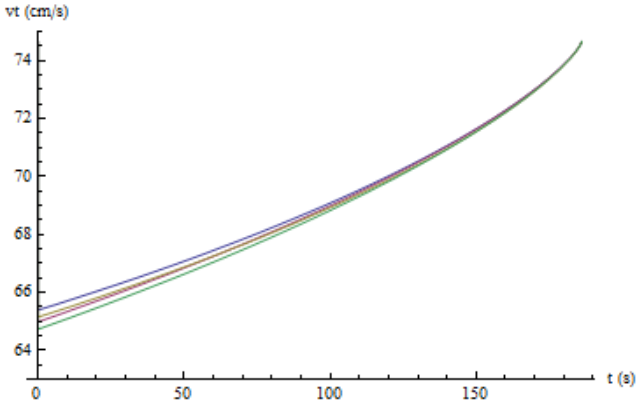

Figure 8 – Transport velocity (cm/s) versus Time (s), for phase $12^{1/4}$" x 5". The green curve drawn is the uncorrected velocity. The pink curve is the corrected velocity by particles concentration effect. The yellow curve is the corrected velocity by wall effect. While the blue curve corresponds to the corrected velocity by both effects.

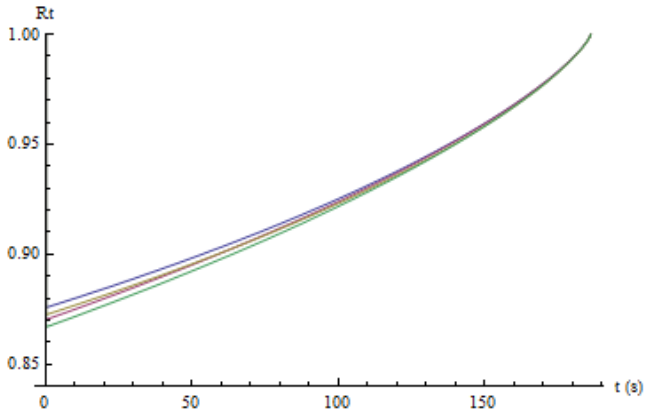

Figure 9 – Transport ratio versus Time (s), for phase $12^{1/4}$" x 5". The green curve drawn is the uncorrected velocity. The pink curve drawn is the corrected velocity by particles concentration effect. The yellow curve drawn is the corrected velocity by wall effect. While the blue curve corresponds to the corrected velocity by both effects.

- Phase $17^{1/2}$" x 5" – 900 GPM

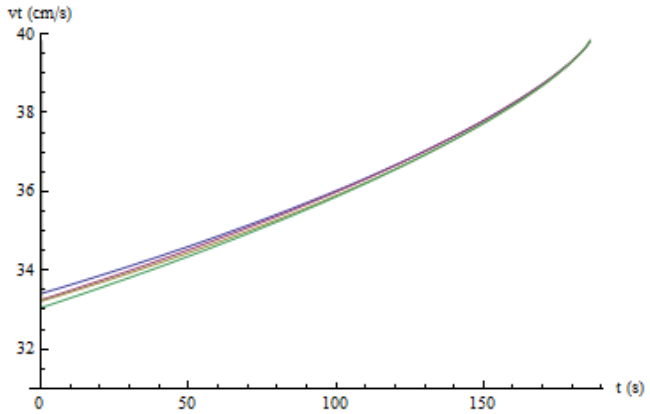

Figure 10 – Transport velocity (cm/s) versus Time (s), for phase $17^{1/2}$" x 5". The green curve drawn is the uncorrected velocity. The pink curve is the corrected velocity by particles concentration effect. The yellow curve is the corrected velocity by wall effect. While the blue curve corresponds to the corrected velocity by both effects.

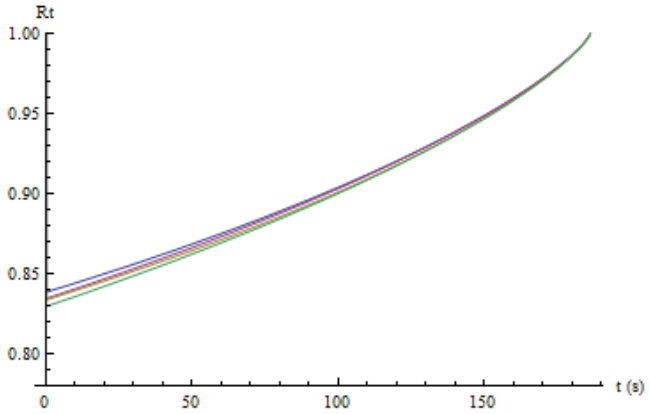

Figure 11 – Transport ratio versus Time (s), for phase $17^{1/2}$" x 5". The green curve drawn is the uncorrected velocity. The pink curve is the corrected velocity by particles concentration effect. The yellow curve is the corrected velocity by wall effect. While the blue curve corresponds to the corrected velocity by both effects.

Results indicate that both the transport velocity and transport ratio increase during the salt particle dissolution, as its settling velocity decreases with time.

Influence of Fluid Viscosity

Figures 12 to 14 illustrate the effect of fluid viscosity on sedimentation velocity, transport velocity and transport ratio during the drilling of a 17 ½ in phase with 900 GPM.

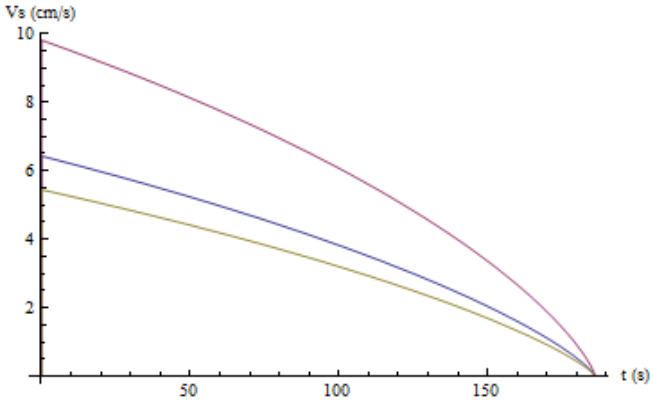

Figure 12 – Settling velocity (cm/s) versus Time (s), varying fluid viscosity. The pink curve drawn is the settling velocity for the lower viscosity fluid (K = 0.8). The yellow curve is the velocity for the higher viscosity fluid (K = 4). While the blue curve corresponds to the velocity for an intermediate viscosity value (K = 2.63).

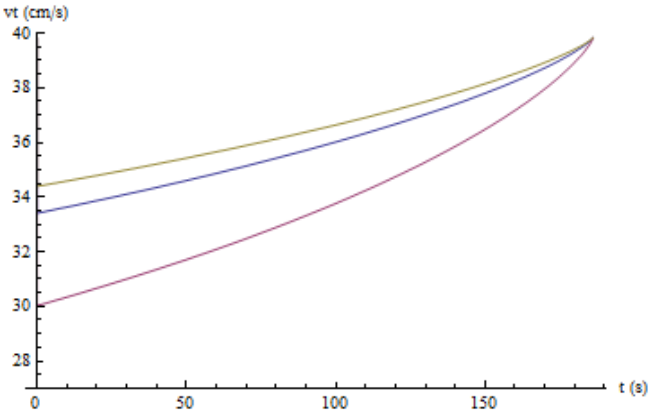

Figure 13 – Transport velocity (cm/s) versus Time (s), varying fluid viscosity. The pink curve drawn is the settling velocity for the lower viscosity fluid (K = 0.8). The yellow curve is the velocity for the higher viscosity fluid (K = 4). While the blue curve corresponds to the velocity for an intermediate viscosity value (K = 2.63).

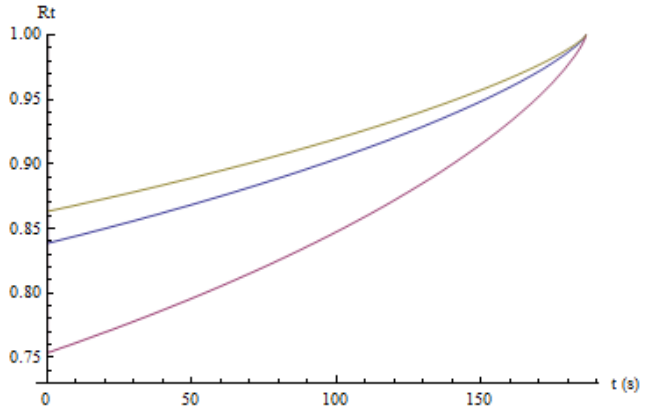

Figure 14 – Transport ratio versus Time (s), varying fluid viscosity. The pink curve drawn is the settling velocity for the lower viscosity fluid (K = 0.8). The yellow curve is the velocity for the higher viscosity fluid (K = 4). While the blue curve corresponds to the velocity for an intermediate viscosity value (K = 2.63).

It could be observed that the particle settling velocity decreases as the fluid viscosity increases. Thus, by using a more viscous fluid it will be obtained a higher transport velocity and, thus, a greater amount of particles will be transported towards the surface. This effect is opposite to the effect of fluid viscosity on particle dissolution. In the end, drag effects are more relevant and fluid viscosity helps cuttings transport as in non-soluble cuttings.

Hydraulics Design Criteria

In this item, based on a maximum annular solids concentration value limit of 5%, ROP limits expansion for a 17 ½ in phase is illustrated for a low viscosity fluid. Otherdata followed table 3.

Solids volumetric concentration was defined as:

$$C_{vt} = \frac{cv}{R_t} \tag{48}$$

Where cv is the solids volumetric concentration generated by the bit, as follows:

$$cv = \frac{ROP * A_{bit}}{ROP * A_{bit} + Q_f} \tag{49}$$

Where ROP is the bit penetration rate and A_{bit} is the cross-sectional area of the bit, which is equal to the cross-sectional area of the well. Salt porosity was considered to be zero.

Figure 15 illustrates the simulation for the 17 in phase. Considering that 5% is the maximum concentration criteria, ROP limits would be pushed to 47 m/h due to salt dissolution. If this effect was neglected, a maximum of 33 m/h would be tolerated. An impressive reduction in drilling time would be achieved.

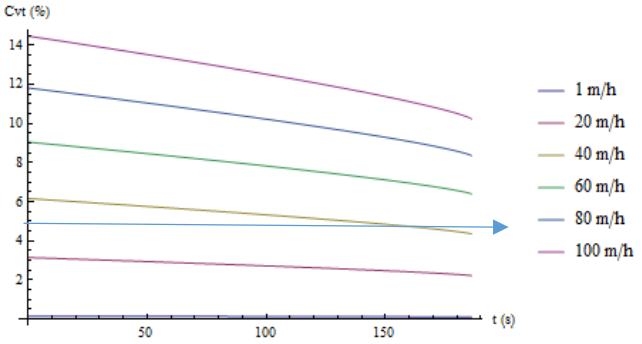

Figure 15 – Solids volumetric concentration in the well (%) versus Time (s).

Conclusions

A comprehensive formulation was proposed to analyze soluble drilled cuttings transport. The formulation is limited to isothermal diluted flows of non-Newtonian fluids. The formulation couples a force balance on a falling solid particle with mass transfer from the particle to the fluid.

A major application for the study is to design salt drilling operations with non-saturated water based fluids. The methodology, incorporating salt dissolution and thus, reduction in particle diameter, allows less conservative criteria for ROP limits.

Further studies including experimental validation, coupling of temperature profiles and the increase in fluid salt concentration due to dissolution will add reliability to predictions.

References

1. Aksel'rud, G.A., Boiko, A.E. & Kashcheev, A.E.: "Kinects of the solution of mineral salts suspended in a liquid flow." UDC 532.73-3. SPE (Society of Petroleum Engineers), 1992.
2. Almeida, O. P.: "Study of the effect of rigid boundaries on the terminal velocity of isometric particles." (in portuguese). Thesis (Master in Chemical Engineering) – Chemical Engineering Program. COPPE/UFRJ, Rio de Janeiro, 1995.
3. Bourgoyne, A. T. et al.: "Applied Drilling Engineering." SPE Text Book Series, v. 2. 2005.
4. Candela, W. F. L.: "A simplified mathematical model for bubble migration in viscoplastic fluids." (in portuguese). Thesis (Master) – Mechanical Engineering Department. Pontifícia Universidade Católica do Rio de Janeiro. Rio de Janeiro, 2013.
5. Coelho, R.M.L. and Massarani, G., "Fluid dynamics of particle: about correlations based in experimental data of Pettyjohn e Christiansen." (in portuguese). Report LSP/COPPE 1/96, 1996.
6. Francis, A.W., "Wall effect in falling ball method for viscosity", Physics, vol. 4, 403-406, 1933.
7. Folsta, M., Resende, E., Dannenhauer, C., Lomba, R., Plucenio, D.: "Use of salt dissolution software to evaluate drilling strategies of massive salt layers," 24345-MS OTC Conference Paper – 2013.
8. Lapple, C.E. and Shepherd, C.B., "Calculation of particle trajectories", IEC, vol. 32, nº 5, 605-617, 1940.
9. Laruccia, M B.: "Particle sedimentation velocity in non-Newtonian fluids: effect of shape and concentration." (in portuguese). Thesis (Master) – Universidade Estadual de Campinas, UNICAMP, Campinas, p.143. 1990.
10. Lomba, R., Pessanha, R., Cardoso Jr., W., Lomba, B., Folsta, M., Gonçalves, J., Teixeira, G.: "Lessons learned in drilling pre-salt wells with water based muds," 24355-MS OTC Conference Paper – 2013.
11. Martins, L. A. A., Calçada, L. A., Scheid, C. M.: "Theoretical and Experimental Study of Dissolution of Salt Particles in Brine Flow." Encontro Nacional de Hidráulica de Poços de Petróleo e Gás, 2C-SPC, Teresópolis, Rio de Janeiro, Brazil, 5-8 August 2013.
12. Massarani, G.: "Fluid dynamics in particulate systems." (in portuguese). Universidade Federal do Rio de Janeiro, Rio de Janeiro, 1997.
13. Munroe (1888), quoted by Fidleris, V. e Whitmore, R.L., "Experimental determination of the wall effect for spheres falling axially in cylindrical vessels", British J. of Applied Physics, vol. 12, 490-494, 1961.
14. Pettyjohn, E.S. and Christiansen, E.B., "Effect of particle shape on free-settling rates of isometric particles", Chem. Eng. Progress, vol. 44, nº 2, 157-172, 1948.
15. Pinto, G. H. V. P.: "Particle dynamics in time dependent viscosity fluids and its application in wells construction." (in portuguese).Thesis (Science and Petroleum Engineering Master) – Science and Petroleum Engineering Program. UFRN, Natal, 2008.
16. Pinto, G. H. V. P.: "A methodology for the evaluation of gas bubble migration in time dependent viscosity fluids and its application in wells construction." (in portugues). Thesis (Science and Petroleum Engineering Doctoral). Universidade Federal do Rio Grande do Norte, Natal, 2012.
17. Richardson, J. F. and Zaki, W. N.: "Sedimentation and fluidization: Tran. Inst. Chem. Eng." n.1, vol. 32, p. 35. 1954.
18. Wilson, S., Driscoll, P., Judis, A., Black, A., Martin, J., Ehgartner, B., Hinkebein, T.: "Drilling salt formations offshore with seawater can significant reduce well costs", SPE 87216 - 2004.